Power Efficient Instrumentation with 100 fA-Sensitivity and 164 dB-Dynamic Range for Wearable Chronoamperometric Gas Sensor Arrays

Haitao Li, Sam Boling and Andrew J. Mason
Electrical and Computer Engineering, Michigan State Univ., East Lansing, MI, USA

Abstract—Chronoamperometric gas sensor arrays show great promise for ultra-low power consumption and low cost for wearable gas sensing devices for human safety and health monitoring. This paper presents a novel power efficient instrumentation circuit with high sensitivity and large dynamic range for wearable chronoamperometric gas sensor arrays. This instrumentation combines an input digital modulation technique and a semi-synchronous incremental ΣΔ ADC structure to achieve very high power efficiency over a large dynamic range with high sensitivity. The proposed instrumentation was implemented in 0.5 µm CMOS technology. Measurement results demonstrate that 164dB cross-scale dynamic range and 100 fA sensitivity are achieved with a high power efficiency.

Keywords—chronoamperometry; gas sensor array; power efficient; wide dynamic range; wearable

I. INTRODUCTION

Air pollution from industrial toxic gas byproducts is a major global contributor to illness and mortality [1], and explosive gases are an increasing threat to occupational and personal safety as energy demands rise. Airborne pollutants and explosive gases vary in both time and space. For example, CO and CH_4 can be released from boilers and stoves in homes, and dangerous levels of CH_4 and SO_2 can be found in underground coal mines [2]. To improve scientific understanding of the health impacts of personal exposure to these pollutants and effectively protect workers throughout the vast underground mine environment, individual wearable devices are desperately needed. Such devices should be of small size, low power, low cost, high sensitivity and able to detect concentrations of multiple gas species.

For the wearable gas sensing application, electrochemical sensor technology possesses several desirable qualities compared with other gas sensor technologies, namely ultra-low power consumption, low cost, good selectivity, and sensitivity to a wide range of gases [3]. Most electrochemical gas sensors are operated in chronoamperometry mode [4, 5]. This electrochemical mode is widely used in commercial gas sensors, to measure gases including O_2, H_2, and toxic compounds such as CO, NO_x, SO_2, etc. The versatility of this technology suggests that an array of electrochemical sensors can simultaneously measure concentration of multiple analyte gases in a wearable device. The low cost, size, and power consumption of modern CMOS technology enables development of suitable instrumentation circuitry for such a wearable gas sensing device, and noise performance would be dramatically improved by integrating sensors directly with the CMOS instrumentation. Substantial research effort has focused on CMOS instrumentations of multi-channel chronoamperometry sensor arrays. Different structures were developed for this purpose, including a sigma-delta (ΣΔ) analog-to-digital convertor (ADC) [6, 7], integration ADC [8], current-to-frequency ADC [9], and hybrid ADC topology [10]. However, none of these existing instruments targeted on amperometric gas sensing array. A wearable amperometric gas sensing array requires instrumentations that simultaneously achieve several performance factors namely: high power efficiency, high sensitivity, and high cross-scale dynamic range from sub-pA to tens of µA. Existing amperometric CMOS instruments cannot meet these requirements simultaneously. As a result, a new amperometric instrumentation approach for wearable amperometric gas sensor arrays is urgently needed.

This paper presents a power-efficient instrumentation with high sensitivity and wide cross-scale dynamic range for wearable amperometric gas sensor arrays. By combining an input current modulation method and high-performance Σ Δ conversion techniques, this circuit achieves 100fA sensitivity and 164 dB cross-scale dynamic range with high power efficiency.

II. APPROACHES AND CIRCUIT ARCHTECTURE

Amperometric gas sensors are biased by a constant DC voltage and generate a DC current at steady state. A wearable amperometric gas sensing array with miniaturized sensors and a ppb-level detection limit requires instrumentation to have sub-pA sensitivity. The gas sensors in the target sensor array generate current levels ranging from sub-pA to several tens of µA. A low-power instrumentation would greatly increase the lifetime of a sensor array system. The compact size of instrumentation is also desired to enable development of multi-channel system. Therefore, a wearable amperometric gas sensing array requires instrumentation designed for compact size, high power efficiency, high sensitivity, and high dynamic range from sub-pA to tens of µA.

A. Analysis of ADC Structures

In a wearable amperometric gas sensing array, the CMOS instrumentation acts to condition and digitize the sensor output current. Among the existing CMOS instrumentations for multi-channel amperometric sensor arrays [6-10], the first-order ΣΔ ADC structure achieves compact size, low (µW) power, and the best sensitivity (fA range) among the techniques surveyed. These structures are promising candidates for wearable gas

This work was supported in part by the National Institute for Occupational Safety and Health (NIOSH) under Grant R01OH009644.

sensor arrays. However, the existing micro-watt ΣΔ ADC structures for amperometric sensor arrays only have high power efficiency for low input current. The digital components consume only 2.4 μA in ref. [6]. For a large input current, the power consumed by digital components does not change substantially, but the analog power consumption increases, largely because the reference current in the ΣΔ structure has to be larger than the input current. When the input current is much larger than 2.4 μA, the reference current of the ΣΔ ADC becomes one of the dominant power dissipation sources and limits the power efficiency. By scaling down a large input current before digitizing it with a ΣΔ ADC, the reference current should be kept small, improving system power efficiency.

B. Current Scaling Approaches and Circuit Architecture

Two approaches show promise for scaling down the input current, namely adjusting the reference current with a current mirror and digital modulation. The current mirror technique is less precise than digital modulation due to device mismatch[7], especially for a scaling ratio much smaller than 1. An analog solution is also less physically compact. As a result, the digital modulation technique was chosen to scale down the input current.

In the digital modulation approach, a precise scaling factor M is obtained by modulating the current with digital pulses of a duty cycle equal to $1/M$. Assuming that the input current is I_{in}, the equivalent average current becomes I_{in}/M after modulation. Because the final stage of a first-order incremental ΣΔ ADC is a counter averaging the frequency modulated signal, this ADC structure is inherently compatible with digital modulation. The effective reference current of such an ADC would be decreased by M times, compared to an unmodulated design. The system level blocks of a ΣΔ ADC employing this modulation technique for current scaling are shown in Fig. 1.

III. Circuit Implementation and Performance Analysis

A. Circuit Implementation

Amperometric sensor output current is delivered from the electrochemical sensor's working electrode (WE) to the instrumentation circuit. The voltage on this electrode must be constant during measurement because the electrochemical sensor has a long settling time (up to several hours) after the DC bias on the WE is changed [3].

The instrumentation with semi-synchronous incremental ΣΔ ADC structure described in [6] achieves fA sensitivity and μW power consumption with a very compact structure. Mismatch between such a circuit's two reference current sources affects the resolution and requires additional calibration [11]. Output current from amperometric gas sensors is a unidirectional signal, generated by either a reduction or an oxidation reaction. As a result, only one reference current source is necessary and was used to complete the circuit's negative feedback. This simplification addresses the reference current mismatch issue. This solution also reduces the current feedback activity and thus reduces total noise and power consumption.

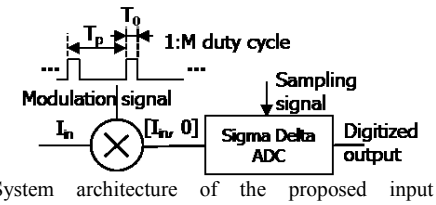

Fig. 1. System architecture of the proposed input modulated instrumentation for wearable amperometric gas sensor arrays.

A switch controlled by a modulation waveform was used to modulate the sensor output current before it flows to the ADC. The current is passed for a single clock cycle and turned off for the followed M-1 clock periods. If the sensor is directly connected to the modulation switch, the sensor's working electrode will float to an indeterminate potential when the modulation switch is turned off. Therefore, a current conveyor was used to maintain a constant voltage on the WE. The current conveyor's transistors are operated in sub-threshold region for sub-μA current consumption, and the power efficiency of this circuit is not compromised when the input current is much larger than 1 μA. For input current at the sub-μA level, the current conveyor is powered of and the input current is directly fed into the unmodulated ΣΔ ADC.

The final implemented circuit is shown in Fig. 2. This circuit is designed for sensors in which current flows out of the working electrode. A cascaded PMOS current mirror with a mirror ratio of 1 was used to maximize current ratio accuracy. For sensors which draw current into the WE, a current conveyor with NMOS current mirror may be used. A bypass signal (BYP) selects between current-modulated and unmodulated operation modes depending on the current levels. All switches are protected from charge injection and clock feed through noise by dummy transistors. Timing diagrams of the clocks controlling circuit operation are shown in Fig. 3. In a modulation cycle, the modulation signal is held high for only one sample cycle to avoid integrator output saturation when I_{in}

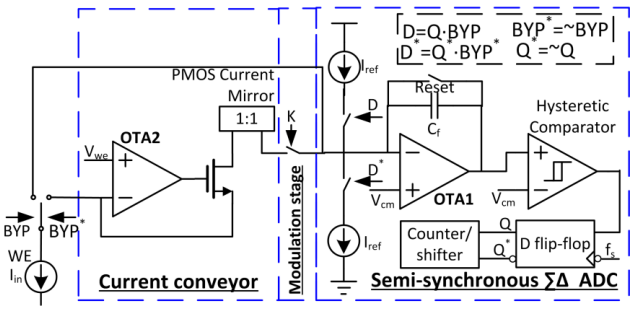

Fig. 2. Simplified blocks of the proposed instrumentation. Switch K is controlled by the modulation signal. I_{in} is the sensor's DC output current. WE is the working electrode of the sensor. V_{we} determines the bias potential held on the WE. f_s is the sampling frequency. The signal BYP* is active for input current above 1 μA and BYP is active when the input current is lower than 1 μA. Only one reference current I_{ref} is active at any time.

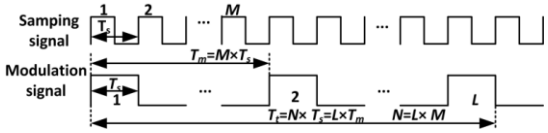

Fig. 3. Control clocks of the input current modulated instrumentation. The reset cycle of the incremental ΣΔ ADC is T_f. The modulator factor is M.

is large.

Let I_{in} be the DC input current and $I_{in}'(t)$ the modulated current. The modulation factor M is equal to the reciprocal of the modulation signal's duty cycle. $I_{in}'(t)$ is expressed by:

$$I_{in}'(t) = \begin{cases} I_{in}, & n \cdot M \cdot T_s \le t < n \cdot M \cdot T_s + T_s \\ 0, & else \end{cases} \quad (1)$$

where n = 0, 1, 2, …; T_s is the sampling signal's cycle. When BYP* is active in Fig. 2, the current is modulated by the modulation stage. The incremental ΣΔ ADC is then governed by:

$$\int_0^{T_t} I_{in}'(t)\,dt = I_{ref} T_s \sum_{i=1}^{N} D_i^* \quad (2)$$

where D_i^* is the modulated digital output of ADC in Fig. 2, controlling reference feedback current I_{ref}; T_t is the reset cycle of the incremental ΣΔ ADC; N is the total digital samples in a reset cycle of the ADC, and $T_t = N \cdot T_s$ is the reset cycle of the ADC.

Substituting (1) into (2) yields

$$I_{in} \cdot L \cdot T_s = I_{ref} T_s \sum_{i=1}^{N} D_i^* \quad (3)$$

where L is the total pulse '1' number of the modulation signal, as identified in Fig. 3. $L \cdot T_s$ equals to the total turned-on time of the modulation stage. Therefore, the transfer function of the current-modulated ΣΔ ADC for a DC input current I_{in} is

$$I_{in} = \frac{I_{ref}}{L} \sum_{i=1}^{N} D_i^* \quad (4)$$

B. Performance Analysis

In (4),

$$\sum_{i=1}^{N} D_i^* \le N \quad (5)$$

and substituting (5) to (4), we have

$$I_{ref} \ge \frac{I_{in}}{M} \quad (6)$$

When M=1, (6) is applied to the unmodulated ΣΔ ADC. Therefore, the reference current source is scaled down M times by the input current modulated ΣΔ ADC.

For a DC input current I_{in}, the minimum power dissipation P_m of the current modulated ΣΔ ADC is approximated by

$$P_m = [\alpha \cdot \min(I_{ref}) + \frac{I_{in}}{M} + I_{b1} + I_{b2} + I_{b3} + I_{digital}]V_{dd}$$
$$= [(\alpha + 1)I_{in}/M + I_{b1} + I_{b2} + I_{b3} + I_{digital}]V_{dd} \quad (7)$$

where I_{b1}, I_{b2}, I_{b3} are the static currents of OTA1, OTA2 and comparator, respectively; $I_{digital}$ represents the total current consumption of digital components; α represents the average duty cycle of D* and satisfies $0 \le \alpha \le 1$. When $I_{in}=I_{ref}/M$, α =1. By biasing transistors in the subthreshold region, I_{b2} and I_{b3} can be operated at sub-μA currents.

To evaluate the power efficiency of the proposed work, the power consumption of modulated and unmodulated ΣΔ ADCs is compared for an equal input current I_{in}. The unmodulated ΣΔ ADCs refers to a semi-synchronous ΣΔ ADC with two reference current sources, same to that in [6]. These two topologies have the same integrator, comparator, D flip-flop and counter/shifter.

Define the reference current in the unmodulated ΣΔ ADC as I_{ref}'.The total power dissipation P_r of the unmodulated design is approximated by

$$P_r = [\min(I_{ref}') + I_{b1} + I_{digital}']V_{dd}$$
$$= (I_{in} + I_{b1} + I_{digital}')V_{dd} \quad (8)$$

where $I_{digital}'$ represents the total current consumption of the ADC's digital components and is approximately 2.4 μA as in [6].

Let I_ε equal $I_{digital}'$ minus $I_{digital}$. Define the power efficiency η as the maximum input current divided by the instrumentation's total current consumption. Compared to the unmodulated ΣΔ ADC, the improved power efficiency $\eta_{improved}$ with input modulation is equal to $(P_r-P_m)/P_m$. When $I_{in} >> |I_{b2}|, |I_{b3}|, |I_\varepsilon|$ and $M >> \alpha+1$ (i.e. $I_{in} >> I_{ref}$), we have

$$\eta_{improve} \approx \frac{I_{in}}{P_m} \quad (9)$$

IV. RESULTS

The input current-modulated ΣΔ ADC for a wearable amperometric gas sensing array system was fabricated in a 0.5 μm CMOS process and is shown in Fig. 4. The capacitor array is controlled by a 4-bit command to maximum circuit performance in different input current ranges. The instrumentation's active area is 0.157 mm^2, allowing integration over 16 channels on a 3×3 mm^2 chip. In test experiments, a GPIB-connected high resolution current source (model 6430 SourceMeter, Keithley Instruments) was used to generate a constant DC current to mimic the sensor output current. A data acquisition card (PCI-6259, National Instruments) was used to provide DC bias voltages to the chip, control the Keithley current source and acquire the digital output of the instrumentation. A FPGA board (Spartan 3E Starter Board, Digilent Inc.) was used to generate control clocks. The whole chip was powered by 5V.

To demonstrate the input current modulated ΣΔ ADC response, the modulation factor M was tested at 1, 2, 4, 8, 16 and 32 to measure the input current ranges. The sampling frequency was set at 100 kHz for all M values except for M=32. When M=32, the sampling frequency was set at 500 kHz to avoid integrator output saturation. Fig. 5 shows a log-linear plot of the normalized digital outputs as a function of input current. The ADC can only measure current from 6 nA to 420 nA with M = 1, which corresponds to no modulation. The

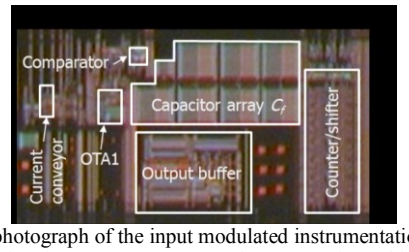

Fig. 4. Chip photograph of the input modulated instrumentation. The output buffer is only for test purpose. After removing this buffer, the instrumentation's active area is 0.157mm^2.

modulation technique expands the ΣΔ ADC maximum input current to 16 µA. As a result, the input current range is improved by 31.7 dB. The maximum input current of the input current-modulated ΣΔ ADC is limited by OTA1's current drive ability and the integrator's output swing. Note that larger *M* shifts the calibration curve to the right, permitting a larger input current level while sacrificing the current detection limit. Increasing the ADC reset cycle time can improve the detection limit for a fixed *M* value. Fig. 6 shows that the sensitivity is as low as 100 fA. As a result, the cross-scale dynamic range of the proposed circuit is 164 dB.

The comparison between this work and other chronoamperometric sensor instrumentations is illustrated in Table I. It shows this work achieves the largest dynamic range, the second best sensitivity and second best power efficiency among designs surveyed.

V. Conclusion

An input current modulated ΣΔ ADC architecture was introduced for wearable chronoamperometric gas sensor arrays. Fabricated in a 0.5 µm technology, the proposed circuit was measured to achieve 100 fA sensitivity and 164 dB cross-scale dynamic range with high power efficiency. These figures were achieved by a novel technique combining digital input current modulation technique and a semi-synchronous incremental ΣΔ ADC structure. By varying the current modulation factor between 1 and 32, the input current range of the instrumentation can be improved by 31.7 dB, compared to unmodulated ΣΔ ADC. The circuit's active area is 0.16 mm^2, allowing over 16 channels on a 3×3 mm^2 chip. This architecture is compatible with more advanced CMOS process technology.

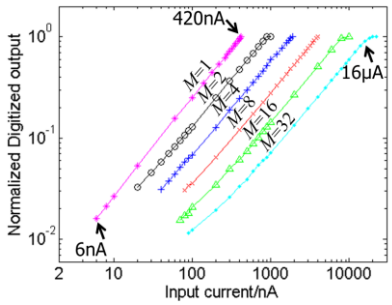

Fig. 5. Calibration curve of the proposed circuit's normalized digitized output for different input currents with different modulation factors *M*. The reference current I_{ref} was fixed at a value in nA range.

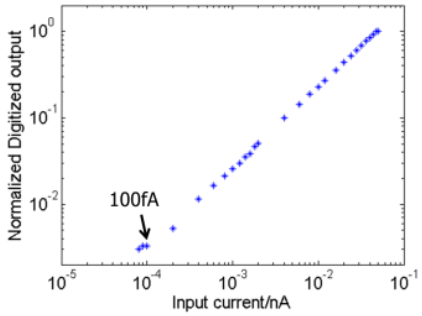

Fig. 6. Calibration curve of the proposed circuit's normalized digitized output for different input currents to evaluate the instrumentation sensitivity. Modulation factor *M* was set at 1. The reference current I_{ref} was set at a value in pA range.

References

[1] R. Brook, "Cardiovascular effects of air pollution," *Clinical Science,* vol. 115, pp. 175-187, 2008.

[2] J. W. Gardner, P. K. Guha, F. Udrea, and J. A. Covington, "CMOS interfacing for integrated gas sensors: A review," *Sensors Journal, IEEE,* vol. 10, pp. 1833-1848.

[3] H. Li, X. Mu, Y. Yang, and A. Mason, "Low Power Multi-mode Electrochemical Gas Sensor Array System for Wearable Health and Safety Monitoring," *Sensors Journal, IEEE* vol. 14, pp. 3391 - 3399, Oct. 2014 2014.

[4] X. Mu, Z. Wang, X. Zeng, and A. J. Mason, "A robust flexible electrochemical gas sensor using room temperature ionic liquid," *Sensors Journal, IEEE,* vol. 13, pp. 3976 - 3981, 2013.

[5] X. Huang, L. Aldous, A. M. O' Mahony , F. J. del Campo, and R. G. Compton, "Toward membrane-free amperometric gas sensors: A microelectrode array approach," *Analytical Chemistry,* vol. 82, pp. 5238-5245, 2010.

[6] A. Gore, S. Chakrabartty, S. Pal, and E. C. Alocilja, "A multichannel femtoampere-sensitivity potentiostat array for biosensing applications," *Circuits and Systems I: Regular Papers, IEEE Transactions on,* vol. 53, pp. 2357-2363, 2006.

[7] M. Stanacevic, K. Murari, A. Rege, G. Cauwenberghs, and N. V. Thakor, "VLSI potentiostat array with oversampling gain modulation for wide-range neurotransmitter sensing," *Biomedical Circuits and Systems, IEEE Transactions on,* vol. 1, pp. 63-72, 2007.

[8] R. Genov, M. Stanacevic, M. Naware, G. Cauwenberghs, and N. Thakor, "16-channel integrated potentiostat for distributed neurochemical sensing," *Circuits and Systems I: Regular Papers, IEEE Transactions on,* vol. 53, pp. 2371-2376, 2006.

[9] M. M. Ahmadi and G. A. Jullien, "Current-mirror-based potentiostats for three-electrode amperometric electrochemical sensors," *Circuits and Systems I: Regular Papers, IEEE Transactions on,* vol. 56, pp. 1339-1348, 2009.

[10] M. H. Nazari, H. Mazhab-Jafari, L. Leng, A. Guenther, and R. Genov, "CMOS neurotransmitter microarray: 96-channel integrated potentiostat with on-die microsensors," *Biomedical Circuits and Systems, IEEE Transactions on,* vol. 7, pp. 338-348, 2013.

[11] C. Yang, S. R. Jadhav, R. M. Worden, and A. J. Mason, "Compact low-power impedance-to-digital converter for sensor array microsystems," *Solid-State Circuits, IEEE Journal of,* vol. 44, pp. 2844-2855, 2009.

TABLE I. Comparison between this Work and other Published Instrumentations for Chronoamperomeric Sensor Arrays

	Max. Current	Sensitivity	Dynamic Range	Power/Chan.	Power Efficiency[1]	Process	ADC structure
TCAS I '06 [7]	100 nA	50 fA	126 dB	11 µW	0.033	0.5 µm	Semi-synchronous sigma-delta
TbioCAS'07 [8][2]	0.5 µA	100 fA	140 dB	1300 µW	0.001	0.5 µm	Feedback modulation sigma-delta
TCAS I '06 [9]	50 µA	46 pA	120 dB	781 µW	0.578	1.2 µm	Integration
TCAS I '09 [10]	1 µA	1 nA	60 dB	70 µW	0.026	0.18 µm	Current to frequency
TbioCAS'13 [11]	350nA	24 pA	95 dB	188 µW	0.006	0.35 µm	Current to frequency + Single slope
This work	**16 µA**	**100 fA**	**164dB**	**241 µW**	**0.331**	0.5 µm	Input modulation sigma-delta

[1] Power efficiency is defined as max. input current divided by circuit's overall consumed current.
[2] For this ref., the circuit's overall consumed current for max. input current was used to calculate power efficiency.